Chinese Chemical Letters 31 (2020) 1690–1693

Contents lists available at ScienceDirect

Chinese Chemical Letters

journal homepage: www.elsevier.com/locate/cclet

Communication

A symmetric aqueous redox flow battery based on viologen derivative

Shuang Liu[1], Meng Zhou[1], Ting Ma, Jian Liu, Qiu Zhang, Zhanliang Tao, Jing Liang*

Key Laboratory of Advanced Energy Materials Chemistry (Ministry of Education), College of Chemistry, Nankai University, Tianjin 300071, China

ARTICLE INFO

Article history:
Received 24 September 2019
Received in revised form 13 November 2019
Accepted 19 November 2019
Available online 21 November 2019

Keywords:
Aqueous redox flow battery
Bipolar redox active molecule
Symmetric redox flow battery
MVI_2
Prohibited crossover problem
High coulombic efficiency

ABSTRACT

Due to the diversity and feasibility of structural modification for organic molecules, organic-based redox flow batteries (ORFBs) have been widely investigated, especially in aqueous solution under neutral circumstance. In this work, a symmetric aqueous redox flow battery (SARFB) was rationally designed by employing a bipolar redox active molecule (*N*,*N*'-dimethyl-4,4-bipyridinium diiodide, MVI_2) as both cathode and anode materials and combining with an anion exchange membrane. For one MVI_2 flow battery, MV^{2+}/ $MV^{\cdot+}$ and I^-/I_3^- serve as the redox couples of anode and cathode, respectively. The MVI_2 battery with a working voltage of 1.02 V exhibited a high voltage efficiency of 90.30% and energy efficiency of 89.44% after 450 cycles, and crossover problem was prohibited. The comparable conductivity of MVI_2 water solution enabled to construct a battery even without using supporting electrolyte. Besides, the bipolar character of MVI_2 battery with/without supporting electrolyte was investigated in the voltage range between −1.2 V and 1.2 V, showing excellent stable cycling stability during the polarity-reversal test.

Redox flow batteries (RFBs) are an attractive electrochemical energy storage technology for large-scale energy storage of renewable sources including wind and solar power generation [1–3]. All-vanadium redox flow battery (VRFB) has already been commercialized and thoroughly investigated since 1980s [4–7]. However, the disadvantages including high cost of vanadium-based active materials, low energy density and acidic operating condition limit the application of VRFBs [8,9]. However, an obvious advantage of VRFB over other traditional RFBs system is that the crossover problem between the anolyte and the catholyte could be prevented effectively by employing the same element of multi-valent vanadium couples (V(II)/V(III)) and (V(IV)/V(V)) in both half-cells.

Inspired by the bipolar feature of VRFBs, symmetric redox flow batteries (SRFBs) emerged [10]. By using only one material possessing bipolar characters, battery system can be simplified drastically, the effort of searching two different materials for both anode side and cathode side can be saved, and the crossover problem existed in non-SRFBs can be effectively prevented [11]. For example, the SRFB with the application of commercially available 2-phenyl-4,4,5,5-tetramethylimidazoleline-1-oxyl oxide (PTIO) can operate at a high cell potential of 2.5 V [12]. By using 5,10,15,20-tetraphenylporphyrin (H_2TPP) as both anolyte and catholyte, a high voltage of 2.83 V and an excellent cycling performance can be achieved by this SRFBs [13]. Although crossover is prohibited and high cell voltage (> 2 V) is achieved in these works, the inflammable and volatile character of organic solvent raises safety issues. In addition, the insufficient solubility of organic molecules, the high-cost and the side reaction restrict the further improvement of non-aqueous RFBs in electrochemical performance. Thus, the symmetric aqueous redox flow batteries (SARFBs) would be one of the most promising directions for future RFBs development [14].

A few SARFBs have been reported so far. Winsberg *et al.* developed a SARFB by use of 2,2,6,6-tetramethylpiperidine-1-oxyl (TEMPO)/Phenazine combi-molecule and achieved a cell voltage of 1.2 V. [14] However, the high-cost of TEMPO limits its large-scale application. Zhu *et al.* reported a SARFB based on 1-(4-ferrocenyl-*n*-butyl)-1′-[3-(trimethylammonio)propyl]-4,4′-bipyridinium cation ($Fc\text{-}bipy^{3+}$), reaching a stable cycle performance of 4000 cycles. Nevertheless, due to the low cell voltage, the theoretical capacity was restricted to 6.7 Ah/L [15]. Viologen compounds are a class of redox active molecules with two redox potentials, which have ever been investigated in some RFBs [16–20]. For instance, Liu *et al.* reported a methyl viologen (MV)/4-hydroxy-2,2,6,6-tetramethyl-piperidin-1-oxyl (4-HO-TEMPO) ARFB with a theoretical energy density of 8.4 Wh/L [21]. However, the side reaction of the 4-HO-TEMPO affects the long term stability. DeBruler *et al.* developed 1,1′-bis(3-sulfonatopropyl)-4,4′-bipyridinium ($(SPr)_2V$)/KI ARFBs

* Corresponding author.
E-mail addresses: liangjing@nankai.edu.cn, lianggrace2001@163.com (J. Liang).
[1] These authors contributed equally to this work.

https://doi.org/10.1016/j.cclet.2019.11.033
1001-8417/

[22]. Nevertheless, the oxidation potential and solubility of catholyte restrict the cell voltage to 1.0 V and the energy density to 6.7 Wh/L. Recently, Luo *et al.* constructed a $(SPr)_2V/Br^-$ based ARFB which possesses a high voltage of 1.51 V [23]. Nevertheless, the crossover issue cannot be prevented. To the best of our knowledge, the application of *N*,*N*'-dimethyl-4,4-bipyridinium diiodide (MVI_2) in a SARFB system has never been reported before.

Here, MVI_2 was synthesized through a one-step methylation reaction, and was introduced to the SARFBs, in which the bipyridinium group acts as the anode redox active material while the iodide ion performs as cathode redox active material (Scheme 1). Cyclic voltammetry (CV) revealed the bipolar character of the obtained organic molecule, with two reversible reactions at potentials of −0.66 V and 0.36 V *versus* Ag/AgCl, respectively. The non-pumped battery exhibited excellent stability and an average coulombic efficiency of 99.30% for 450 cycles. When tested in the voltage range between −1.2 V and 1.2 V, the battery showed a stable polar-reversal performance. MVI_2 demonstrated its capability as a bipolar redox-active material in subsequent multiple polarity reversals.

Earlier research showed that the divalent viologen cation (MV^{2+}) can undergo a two-step reduction to the neutral viologen (MV^0). [24] Generally, the first reduction to the monovalent radical cation ($MV^{\cdot+}$) is fully reversible, while the second step may lead to the side reactions or precipitation due to the decreased solubility of the reduction product. The $MV^{\cdot+}$ formed when the MV^{2+} was reduced during the charge process, and the reaction went inversely upon the discharge process. The redox reaction happened on the anode side exhibited satisfied reversibility. Considering that $MV^{\cdot+}$ is sensitive to oxygen, the oxygen sensitive character can be used to prove the formation of the charged product on the anode side. UV–vis spectroscopy was applied to detect the characteristic peak of the $MV^{\cdot+}$ (Fig. S1 in Supporting information). The measurement was carried out and the testing result was collected every two minutes to get series of consequences. With time passing by, the strength of explored peak at both 395 nm and 605 nm declines gradually, while the peak appears at 257 nm increases accordingly. At the very end, the former two peaks vanished and the later peak strengthened to a maximum value, and the spectral peak return to the same with its original state. The visualized change of solution color from violet to transparent yellow also evidenced the oxidation process of the $MV^{\cdot+}$ into the MV^{2+} (insets of Fig. S1).

To avoid occurrence of the irreversible second-step reduction reaction, CV was carried out in the potential range from −0.85 V to 0.60 V. Note that the reduction of divalent viologen cation into monovalent radical cation takes place at −0.70 V and the oxidation occurs at −0.63 V (Fig. 1). For the cathode side, oxidation of I^- into I_3^- takes place at 0.48 V and reduction of I_3^- into I^- occurs at 0.24 V. This in total gives the symmetric system a theoretical cell voltage of 1.02 V, that is much higher than that of Fc-bipy^{3+}-based SARFBs (0.7 V) [15] and comparable with that of the MV/ferrocene ARFB (1.05 V) [25] and $(SPr)_2V$/KI ARFB (1.0 V) [22]. With this voltage, a theoretical energy density of 8.0 Wh/L can be achieved, which is comparable with that of the MV/4-HO-TEMPO (8.4 Wh/L) [21] and $(SPr)_2V$/KI ARFBs (6.7 Wh/L) [22]. CV at varied scan rates from 10 mV/s to 100 mV/s showed that the peak potentials of both oxidation and reduction of anode material remain almost unchanged (Fig. S2 in Supporting information), indicating an outstanding reversibility of MVI_2 as anolyte. For the cathode side, only negligible peak shift can be observed with the increase of the scan rate. Furthermore, for both the anode and the cathode, the peak current follows a strict linear trend with the rise of square root of the scan rate for both the oxidation and reduction reaction (Fig. S3 in Supporting information). These results imply an excellent electrochemically reversible redox-reaction and a diffusion-controlled process [26].

Further kinetic investigation on anode side were performed *via* rotating disk electrode (RDE) measurements with rotation rates in the range of 0 rpm–2500 rpm (Fig. 2a). Limiting current gradually increased with the increase of square root of rotation speed. Levich analysis showed good linear relation between limiting current under different rotation rates and the boost of square root of rotation speed at −0.85 V *versus* Ag/AgCl (Fig. 2b), indicating a diffusion-controlled behavior of viologen cation. The diffusion coefficient was calculated to be 3.10×10^{-6} cm^2/s, which is at typical magnitude for organic compounds reported in most of the previous research [21,27,28]. Further analysis with the application of Koutecký-Levich equation [15], provided the mass-transfer

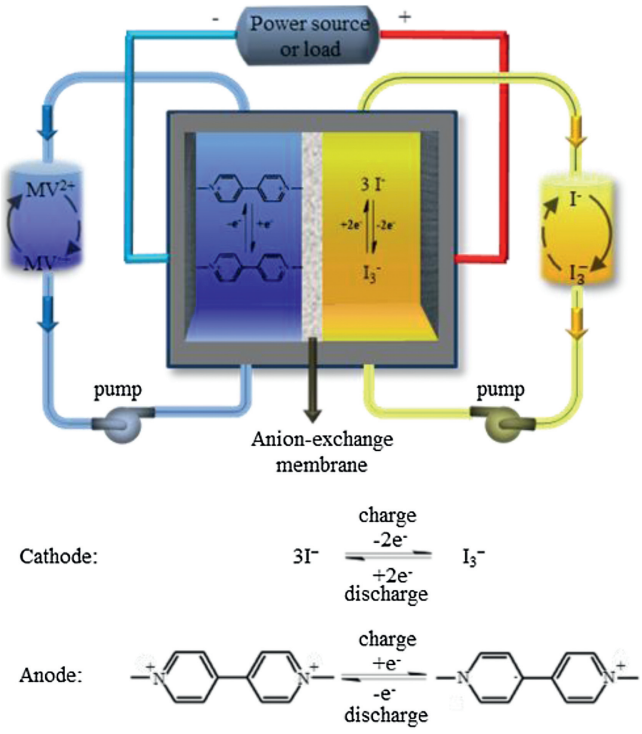

Scheme 1. Working sketch of the aqueous MVI_2 redox flow battery and the theoretic redox mechanism for both anode and cathode.

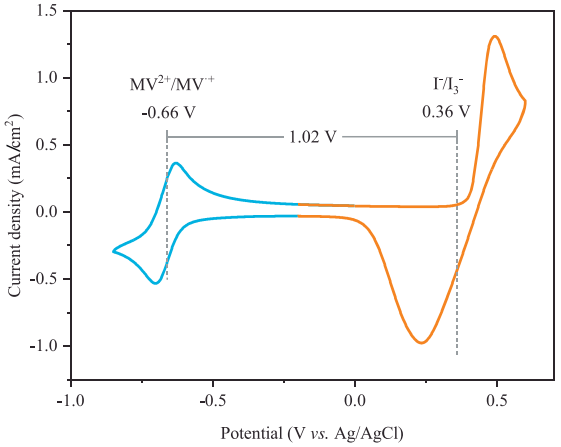

Fig. 1. Cyclic voltammetry of *N*,*N*'-dimethyl-4,4-bipyridinium diiodide at a scan rate of 100 mV/s. Condition: 2 mmol/L MVI_2 and 1 mol/L NaCl in 20 mL deionized water, glassy carbon working electrode, platinum plate counter electrode, Ag/AgCl reference electrode.

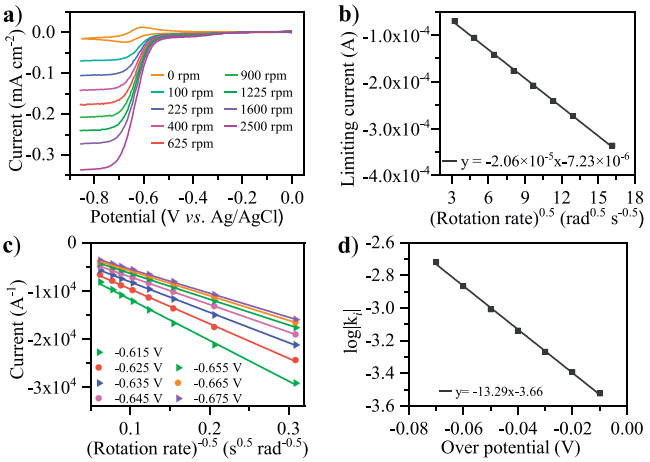

Fig. 2. Results of rotating disk electrode experiments of MVI_2. (a) RDE voltammograms under different rotating speed. (b) The limiting current (at −0.85 V *versus* Ag/AgCl) *versus* the square root of the rotation velocity (Levich plot), (c) Koutecký-Levich plot and (d) Tafel plot with varied overpotential. Measured at a concentration of c_0 = 2 mmol/L MVI_2, in 0.1 mol/L NaCl(aq).

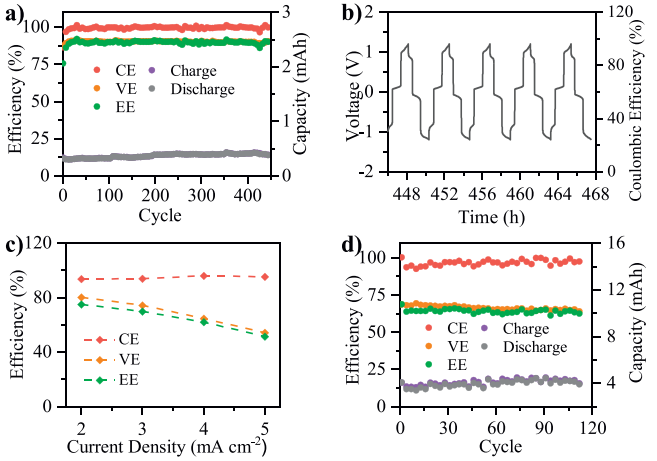

Fig. 3. Electrochemical performance of MVI_2 redox flow battery test. (a) Long-term cycling performance (0.2 V to 1.2 V) of a non-pumped battery at a constant current density of 2 mA/cm^2, concentration of active material c_0 = 0.05 mol/L, in 1 mol/L NaCl(aq). (b) Polarity-reversal test of the symmetric redox flow battery. (c) Coulombic, voltage and energy efficiency of a flow cell depending on the applied current density from 2 mA/cm^2 to 5 mA/cm^2. (d) Cycling performance (0.2 V to 1.2 V) of a flow battery at a current density of 4 mA/cm^2. Concentration of active material c_0 = 0.1 mol/L, in 1 mol/L NaCl(aq).

independent current i_k (Fig. 2c). The linear fit of log|i_k| *versus* overpotential yielded the exchange current i_0 (Fig. 2d). According to Nicholson's method [29], the calculated electron transfer rate constant (k^0) is calculated to be 0.69 cm/s, which is higher than some other organic active materials in ARFBs [14,15].

Ion conductivity test showed that the water solution of MV-based organic salt exhibits excellent conductivity (0.5 mol/L MVI_2, 51.5 mS/cm, 25 °C), which is acceptable compared with that of sodium chloride solution (1 mol/L NaCl, 87.5 mS/cm, 25 °C), implying a high mobility of anion counter ions of MV^{2+}. In this way, it is possible to construct a battery system without the supporting electrolyte NaCl. To confirm the feasibility of NaCl-free SARFB system, non-pumped cell was made using 0.1 mol/L MVI_2(aq) without introduction of NaCl. Electrochemical tests firstly evidenced that the battery worked properly for 200 consecutive cycles with average coulombic efficiency of 98.46% (Figs. S4a and b in Supporting information). The decay of the capacity after first cycle (Fig. S4b) is due to the unbalanced state of solution, which resulting in the second step reaction of viologen. With the charge and discharge going on, the solution tends to balance, and the second step reaction of viologen vanished, resulting in the capacity decay (Fig. S4c in Supporting information). The increased polarization of the charge/discharge curves caused by the void of supporting electrolyte decreases the voltage efficiency of the battery, which in return reduces the energy efficiency. In this sense, supporting electrolyte needs to be introduced for further investigation.

To optimize the best supporting electrolyte, charge/discharge curves under different sodium salt conditions are performed (Fig. S5 and Table S1 in Supporting information). It can be concluded that 1 mol/L NaCl can provide better electrochemical performance, other electrolytes preferred in published research exhibited side reactions and/or increased polarization of the charge/discharge behaviour. Therefore, 1 mol/L NaCl was filtered as the supporting electrolyte. The solubility of MVI_2 in 1 mol/L NaCl aqueous solution was also checked by UV–vis absorbance spectra (Fig. S6 in Supporting information). It can be calculated that the saturation concentration of MVI_2 in 1 mol/L NaCl aqueous solution is 0.40 mol/L and lower than that in pure water (0.58 mol/L, Fig. S7 in Supporting information) due to salting out. Besides, to determine the suitable concentration of MVI_2 in cells, non-pumped cells were constructed (Fig. S8 in Supporting information) using MVI_2 with different concentrations in 1 mol/L NaCl aqueous solution as electrolyte, respectively. After tested at a constant current density of 2 mA/cm^2 and a voltage range from 0.2 V to 1.2 V, cells with 0.05 mol/L MVI_2 reached the most stable cycle performance (Fig. 3a). However, MVI_2 with higher concentrations provided poor cycle performance or low capacity (Fig. S9 in Supporting information). Besides, precipitation occurred with 0.1 mol/L MVI_2 in 1 mol/L NaCl(aq) (Fig. S10 in Supporting information). Because extra introduction of NaCl may decrease the solubility of the more hydrophobic and reduced monovalent viologen radical cation. Therefore, 0.05 mol/L is the most suitable concentration of MVI_2 1 mol/L NaCl aqueous solution for battery operation.

According to the long-term cycling test of the non-pumped battery, the proper range of the working potential can be investigated. As shown in Fig. 3a, the battery with 0.05 mol/L MVI_2 active material as the electrolyte exhibited an excellent stability and an average coulombic efficiency of 99.30% for 450 cycles. Although there was a capacity increasing in previous cycles due to the membrane and electrode activation process, an overall excellent performance can still be obtained. The small polarization of charge/discharge curves gives the battery an average voltage efficiency of 90.07%, thus a high average energy efficiency of 89.44% is obtained. The above 99% coulombic efficiency can be regarded as an indicator of the prevention of crossover problem [30]. It is worth noting that there was no colour change in catholyte after charge/discharge process and the original transparent yellow was maintained after 450 cycles (Fig. S11 in Supporting information), suggesting that the crossover problem was prohibited as well. Attempt on polarity-reversal test of non-pumped symmetric RFBs was investigated according to the following process, the assembled cell was charged/discharged in the voltage range of 0.2 V to1.2 V for ten cycles, and then the charge/discharge voltage was reversed in the range of −1.2 V to −0.2 V. The battery can work stably for more than 500 h (Fig. S12 in Supporting information). Further investigation of fully polarity-reversal test was implemented in a voltage window of −1.2 V to 1.2 V for 100 cycles, achieving a high average coulombic efficiency of 99.93%. In addition, water electrolysis was avoided completely (Fig. 3b and Fig. S13 in Supporting information).

Flow battery was further investigated combining 0.1 mol/L active material (MVI_2) with 1 mol/L supporting electrolyte (NaCl). The battery was tested at varied current density from 2 mA/cm^2 to 5 mA/cm^2 to give further investigation of the electrochemical performance. As shown in Fig. 3c, a high energy efficiency of 74.94% can be achieved at a low current density of 2 mA/cm^2, even at a current density of 5 mA/cm^2, the energy efficiency still exceeds 51.46%. Long-term cycling test of the flow battery was measured at a constant current of 4 mA/cm^2 and a voltage range from 0.2 V to 1.2 V (Fig. 3d). The capacity was able to reach up to 3.33 mA h, higher than that in non-pumped battery with the same MVI_2 concentration (Fig. S9a). Moreover, the flow battery showed a capacity retention of 98.96% after 100 cycles charge/discharge test, higher than some other viologen-based RFBs [31], though it still remains to be improved. The fluctuation of electrochemical result observed in Fig. 4d during the flow battery test may attribute to the electrolyte when circulated through a peristaltic pump. Some inevitable jitters and temperature variation will cause the data to fluctuate as well. Although the overall electrochemical performance of this MVI_2-based-SARFB battery remains to be improved, the use of cheap and benign NaCl electrolyte and the low cost AHA anion exchange membrane reduces the total capital cost compared with nafion series membranes (*e.g.*, nafion-115, 117, 212), and the combination achieves better capacity than nafion-based batteries (Fig. S14 in Supporting information) and shows comparative energy efficiency compared with some similar works [16,21,25]. This design provides an effective strategy to solve the crossover problems of ARFBs, and points out the direction for the development of green and low-cost SARFBs simultaneously. It can be expected that if the concentration of MVI_2 can be enhanced through molecule modification, there will be much outstanding electrochemical behaviours of SARFBs.

In conclusion, the abovementioned bipolar redox active material MVI_2 was synthesized through a simple one-step methylation reaction, with a high yield of more than 95%. For the first time the small organic molecule with both cathodic and anodic redox active centers were applied for symmetric aqueous redox flow batteries and its bipolar character was investigated. Based on the fact that the organic salt possesses excellent conductivity which is even comparable to that of sodium chloride, battery test using only MVI_2 solution without any supporting electrolyte evidenced our hypothesis of constructing a system without supporting electrolyte. The non-pumped battery tested from 0.2 V to 1.2 V exhibited high voltage efficiency of 90.07%, high energy efficiency of 89.44%, and high coulombic efficiency of 99.30%. The crossover problem is prevented to some extent. Electrochemistry tests exhibit a well polar-reversal capability of the bipolar characterized MVI_2, with a rather stable performance of an average coulombic efficiency of 99.93% during charge/discharge in the voltage range from −1.2 V to 1.2 V. Flow battery achieved a good performance with higher concentration of active material compared with non-pumped battery. This design is also an inspiration for other SARFBs.

Declaration of competing interest

The authors declare that they have no known competing financial interests or personal relationships that could have appeared to influence the work reported in this paper.

Acknowledgments

This work was supported by the National Key R&D Program of China (Nos. 2016YFA0202500 and 2016YFB0901502), the National Natural Science Foundation of China (NSFC, Nos. 21673243, 51771094 and 21805141), the Ministry of Education (MOE) of China (No. B12015) and Tianjin High-Tech (No. 18JCZDJC31500).

Appendix A. Supplementary data

Supplementary material related to this article can be found, in the online version, at doi:https://doi.org/10.1016/j.cclet.2019.11.033.

References

[1] G.L. Soloveichik, Chem. Rev. 115 (2015) 11533–11558.
[2] M. Park, J. Ryu, W. Wang, J. Cho, Nat. Rev. Mater. 2 (2016) 16080–16098.
[3] Z. Yuan, H. Zhang, X. Li, Chem. Commun. (Camb.) 54 (2018) 7570–7588.
[4] M. Skyllas-Kazacos, R. Robins, U.S. Patent, No. 4786567, 1986.
[5] M. Skyllas-Kazacos, M.H. Chakrabarti, S.A. Hajimolana, F.S. Mjalli, M. Saleem, J. Electrochem. Soc. 158 (2011) R55–R79.
[6] E. Sum, M. Skyllas-Kazacos, J. Power Sources 15 (1985) 179–190.
[7] M. Skyllas-Kazacos, M. Rychcik, R.G. Robins, A.G. Fane, M.A. Green, J. Electrochem. Soc. 133 (1986) 1057–1058.
[8] Á. Cunha, J. Martins, N. Rodrigues, F.P. Brito, Int. J. Energy Res. 39 (2015) 889–918.
[9] M. Skyllas-Kazacos, G. Kazacos, G. Poon, H. Verseema, Int. J. Energy Res. 34 (2010) 182–189.
[10] P.G. Rasmussen, US Patent, No. 8080327 B1, 2011.
[11] R.A. Potash, J.R. McKone, S. Conte, H.D. Abruña, J. Electrochem. Soc. 163 (2016) A338–A344.
[12] W.T. Duan, R.S. Vemuri, J.D. Milshtein, et al., J. Mater. Chem. A Mater. Energy Sustain. 4 (2016) 5448–5456.
[13] T. Ma, Z. Pan, L. Miao, et al., Angew. Chem. Int. Ed. 57 (2018) 3158–3162.
[14] J. Winsberg, C. Stolze, S. Muench, et al., ACS Energy Lett. 1 (2016) 976–980.
[15] Y. Zhu, F. Yang, Z. Niu, et al., J. Power Sources 417 (2019) 83–89.
[16] T. Janoschka, N. Martin, M.D. Hager, U.S. Schubert, Angew. Chem. Int. Ed. 55 (2016) 14427–14430.
[17] K. Murugavel, Polym. Chem. 5 (2014) 5873–5884.
[18] Y. Gu, W. Hong, W. Choi, et al., J. Electrochem. Soc. 161 (2014) H716–H721.
[19] C. DeBruler, B. Hu, J. Moss, et al., Chem 3 (2017) 961–978.
[20] B. Hu, Y. Tang, J. Luo, et al., Chem. Commun. (Camb.) 54 (2018) 6871–6874.
[21] T.B. Liu, X.L. Wei, Z.M. Nie, V. Sprenkle, W. Wang, Adv. Energy Mater. 6 (2016) 1501449–1501457.
[22] C. DeBruler, B. Hu, J. Moss, J. Luo, T.L. Liu, ACS Energy Lett. 3 (2018) 663–668.
[23] J. Luo, W.D. Wu, C. Debruler, et al., J. Mater. Chem. A Mater. Energy Sustain. 7 (2019) 9130–9136.
[24] C.L. Bird, A.T. Kuhn, Chem. Soc. Rev. 10 (1981) 49–82.
[25] B. Hu, C. DeBruler, Z. Rhodes, T.L. Liu, J. Am. Chem. Soc. 139 (2017) 1207–1214.
[26] J. Winsberg, C. Stolze, A. Schwenke, S. Muench, M.D. Hager, U.S. Schubert, ACS Energy Lett. 2 (2017) 411–416.
[27] A. Orita, M.G. Verde, M. Sakai, Y.S. Meng, Nat. Commun. 7 (2016) 13230–13238.
[28] K. Lin, Q. Chen, M.R. Gerhardt, et al., Science 349 (2015) 1529–1532.
[29] R.S. Nicholson, Anal. Chem. 37 (1965) 1351–1355.
[30] J. Winsberg, T. Hagemann, T. Janoschka, M.D. Hager, U.S. Schubert, Angew. Chem. Int. Ed. 56 (2017) 686–711.
[31] B. Hu, T.L. Liu, J. Energy Chem. 27 (2018) 1326–1332.